Journal of Applied Polymer Science

Preparation, Property Characterization and UV-Converting Application of Poly(conjugated azomethine-urethane)/Hydroxyl Polyacrylate Resin

Can-Pei Liu, Man-Kai Wang, Quan Xiao
College of Materials Science and Engineering, Fujian Key Laboratory of Polymer Materials, Fujian Normal University, 350007 Fuzhou, Fujian, People's Republic of China
Correspondence to: C.-P. Liu (E-mail: lcpcorey@fjnu.edu.cn)

ABSTRACT: A functional polyurethane coating with ultraviolet (UV) rays converting ability of changing higher energy UV rays into lower ones was prepared from poly(conjugated azomethine-urethane) (CAUP) reacting with hydroxyl polyacrylate resin (HPAR). As an oligomeric isocyanate, CAUP was prepared in a reaction of toluene-2,4-diisocyanate with *N*,*N*′-bis(4-hydroxyl-3-methoxybenzylidene)-*o*, *m* or *p*-diaminobenzene that was synthesized from vanillin and *o*-phenylenediamine or *m*-phenylenediamine or *p*-phenylenediamine. Fourier transform infrared spectroscopy, ^{1}H-NMR, UV–vis, and fluorescence spectra were used to characterize those synthesized products and HPAR/CAUP films. UV-converting abilities of HPAR/CAUP films had been demonstrated by natural exposure to ageing and the fluorescence emission spectra of HPAR/CAUP films and CAUP solutions. Red-shift phenomena in the fluorescence emission spectra were due to molecule aggregations and stacks caused by intramolecular and intermolecular interactions such as hydrogen bonding effects. Dynamic mechanical thermal analysis and thermogravimetric analysis techniques were employed to study their mechanical and thermal properties of HPAR/CAUP films. The films exhibited excellent mechanical properties and owned high glass transition temperatures over 97.0°C, and their maximum thermal degradation temperatures were about 176.0°C. © 2013 Wiley Periodicals, Inc. J. Appl. Polym. Sci. 129: 3629–3639, 2013

KEYWORDS: spectroscopy; polyurethanes; properties and characterization; thermal properties; ageing

Received 9 October 2012; accepted 3 February 2013; published online 1 March 2013
DOI: 10.1002/app.39111

INTRODUCTION

Polymers containing poly-aromatic rings or conjugated $\pi-\pi$ bonds have still been an active study field due to their potential applications as photoluminescence material. Aldehyde reacting with a primary amine gives a condensation reaction product containing an azomethine (—CH=N—) linkage. Polymers containing azomethine linkages and $\pi-\pi$ conjugated bonds are species of both proton donor and proton acceptor.[1–3] Issam and Ismail[4] and Bajsic and Rek[5] reported that thermal stabilities of those polymers had been improved since they contained C=C and C=N conjugated segments in molecular backbones. Kaya et al.[6] found that physical changes of the poly(azomethine-urethane)s including melamine linkages prepared from aromatic hydroxyaldehydes and toluene-2,4-diisocyanate (TDI) were thermally stable up to 230–240°C.

Polyurethane coatings are widely used in many fields thanks to their excellent comprehensive properties such as excellent mechanical properties and protective properties, and so forth. Polyurethanes coatings, for example, have a wide range of applications in furniture, train, automotive car, plastics, household appliances, constructions and other industrial fields.[6] By changing a hard segmental component that contained —NCO functional group, or by changing a soft segmental component that contained —OH functional group, the hard-soft-two-component polyurethane coatings with various kinds of properties had been produced. Hydroxyl polyacrylate resin (HPAR) is a transparent functional polymer that has resistance to ultraviolet (UV) rays and does not absorb in the visible light range.[7] Because HPAR has excellent hardness, gloss, flexibility and adhesive to substrate materials, various kinds of HPARs are manufactured and applied in the coating industry. If HPAR is used as a soft segmental component, and an oligomeric isocyanate precursor that contains —NCO functional groups, C=C and C=N conjugated bond segments in its molecular backbone is used as a hard segmental component, a kind of polyurethane coating can be prepared in a mentioned way and it may have good thermal stabilities and/or other functional abilities. For instance, the palm-based acrylic polyol ester resin could be used as a UV curable coating.[8] The hybrid polymer coating film of acrylic polyol/hexamethylene diisocyanate (HDI)/nano-$CaCO_3$ had improved its gloss, pencil hardness, abrasion resistance.[9]

Applied Polymer SCIENCE

During our previous application tests of HPAR/HDI coatings in the Qing-Zang plateau in China, under the natural exposure to ageing in Lhasa and accelerated 254 and 313 nm UV ageing in the years from 2004 to 2007, we found that UV severely affected the film to age and that its gloss of HPAR/HDI film exponentially decayed under UV irradiation.[7] HPAR/HDI films had excellent anti-photodegradation and anti-photo abilities and it could be used in severe UV irradiation areas in the Qing-Zang plateau. However, in their practical application in the Qing-Zang plateau, some of the color coatings, like the red or phthalocyanine blue color coating films, would be fast deteriorated so that their decoration would be quickly faded or lost. This was due to their shortcomings of photodegradation and photo and also due to the fact that the temperature at the surface of the decorative or protective coating films might be greatly increased under the severe UV irradiation for a certain time. Although many studies reported that anti-photodegradation and anti-photo additives, and light-stabilizers like radical scavengers as well the hindered amine light-stabilizers or strong absorbers of UV solar radiation,[10–12] could increase coatings resistance to weathering, the anti-photodegradation and anti-photo abilities of coating films mainly depended on the matrix polymer in the coatings. Even though these light-stabilizers had been used in the coatings, our applications proved that some of the additives had not enough resistance to weathering. In fact, to protect steel, wood, or train out-carriage protective materials and so on against higher energy irradiation of UV rays, many researchers and engineering technicians had made great efforts in the past many years. It is a good idea to find a way in converting those higher energy UV rays to some lower ones. Unfortunately, there was not a study of polyurethane/HPAR on a UV-converting coating. HPAR/HDI coating has not this converting functional ability although it can be used as a finish coating film in severe UV irradiation areas. However, if some transparent polyurethane coatings, which are compatible with HPAR/HDI coatings, can be used as a middle part of the film to change higher energy UV rays into some lower energy ones, the decoration and protection and the natural life of the coating film in the severe UV irradiation areas will be prolonged. Hence, to the end to protect the steel, wood, or train out-carriage and so on in the Qing-Zang plateau from severe UV irradiations, it is necessary for one to develop some transparent and highly thermal stable polyurethane coatings with UV rays converting ability. For example, a certain polyurethane-polyacrylate coating that has high enough thermal degradation temperature and does not absorb or absorbs as little as possible in visible light range, which may keep the decorative material color being clearly seen, may be a good choice.

In this work, *N*,*N*′-bis(4-hydroxyl-3-methoxybenzylidene)-*o*, *m* or *p* (1,*n*)-diaminobenzene (Compound A, $n = 4$, *p*-isomer; Compound B, $n = 2$, *o*-isomer; or Compound C, $n = 3$, *m*-isomer) was prepared by a classical condensation reaction of *o*-phenylenediamine or *m*-phenylenediamine or *p*-phenylenediamine with 4-hydroxyl-3-methoxybenzaldehyde (vanillin). Then, Compound A, B, and C respectively reacted with TDI by a step-growth polymerization reaction mechanism to yield the poly(conjugated azomethine-urethane) (CAUP, CAUP-A, CAUP-B, or CAUP-C, Scheme 1), which contained —CH=N— and urethane linkages in its molecular backbone.

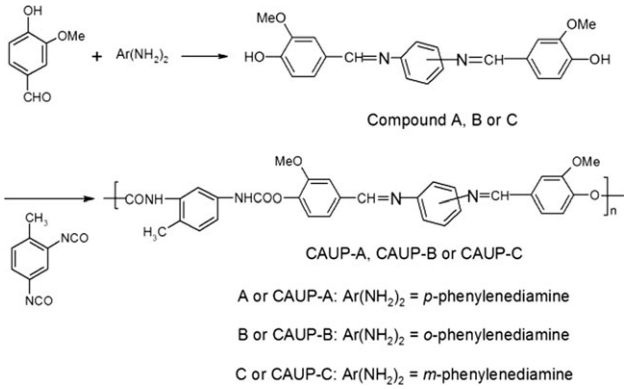

Scheme 1. Synthesis of the poly(conjugated azomethine-urethane).

Although the molecular rigidity of CAUPs seems to be great, the X-ray diffraction data indicate that the three CAUPs are all amorphous. And rheological analysis shows that these CAUPs have good processing properties for making films. The principles of polymer chemistry and physics tell us that amorphous polymer generally has good processing properties for making a film. Thus, the transparent polyurethane coatings can be prepared based on CAUPs as oligomeric isocyanate precursors to react with HPAR. The complex color film of HPAR/CAUP with a UV-converting ability was also prepared. As candidate films, those complex red or blue HPAR/CAUP films had been applied to natural exposure to in Lhasa for more than 9 months. Consequently, the anti-photodegradation and anti-photo abilities of the complex red or blue films were compared with that of the pure HPAR/HDI film.

To develop UV converting functional coating, we characterized the three synthesized poly(conjugated azomethine-urethane)s and their functional abilities of HPAR/CAUP coating films. Fourier transform infrared spectroscopy (FT-IR) and H-nuclear magnetic resonance (^{1}H-NMR) spectrum were employed to characterize Compound A, B, and C. FT-IR, UV visible spectroscopy (UV–vis), thermogravimetric analysis (TGA) and dynamic mechanical thermal analysis (DMTA) techniques were used to investigate the coating films of HPAR/CAUPs, and the fluorescence spectra of the dilute solutions of CAUPs in *N*,*N*-dimethylformamide (DMF) and the coating films of HPAR/CAUPs were also studied.

EXPERIMENTAL

Materials

All the chemicals in this work were analytical grade reagents. Vanillin, *o*-phenylenediamine, *m*-phenylenediamine, *p*-phenylenediamine, TDI (purity is over 99.9%, TDI-100, 2,4-isomer), methacrylic acid, methyl methacrylate, butyl acrylate, 2-hydroxylethyl acrylate, 2-hydroxylpropyl acrylate, benzoyl peroxide, ethyl acetate, anhydrous ethanol, and DMF were purchased from Sinopharm Chemical Reagent. DMF was distilled under reduced pressure before use. Unless otherwise indicated, the others were used without further purification treatments. HPAR

Table I. Property of HPAR

HPAR	Value
NV (%)	50 ± 2
OH (%)	1.7
Glass transition temperature (T_g)(°C)	30.8
M_n (10^3 g·mol^{-1})	9.09
Molecular weight distribution (M_w/M_n)	1.86

was prepared based on our former method[7] by copolymerizing methacrylic acid, methyl methacrylate, butyl acrylate, 2-hydroxylethyl acrylate and 2-hydroxylpropyl acrylate. HPAR was dissolved in DMF for use. The —OH functional group contents based on nonvolatile (NV) and other properties of HPAR were listed in Table I.

PROCEDURES

Preparation of Compound A, B, and C

15.20 g (0.10 mol) of vanillin, 5.40 g (0.050 mol) of *p*-phenylenediamine and 70 mL of anhydrous ethanol were put into a flask, and then the reaction mixture was stirred under reflux. During the reaction, some obvious color change of the reaction mixture solution or some color precipitate in the flask indicated that a condensation reaction was taking place. After refluxing for 6 h, a mass of yellow precipitate (Compound A) was formed. After recrystallization from ethanol/DMF (1 : 1), its yield was weighed to be 74%. Melting-point (mp) of Compound A was 194.1–194.4°C that was measured with a digital mp apparatus (WRS-1B, Shanghai precision & scientific, China). FT-IR spectrum of Compound A was shown in Figure 1(a).

^{1}H-NMR [deuterated dimethyl sulfoxide (DMSO-d_6), the chemical shift (δ) in ppm, shown in Figure 1(d)] of Compound A: 9.752 (s, 2H, ArOH), 8.511 (s, 2H, N=CH), 7.540 (d, $J_{a\text{-}b}$ = 1.6 Hz, 2H; ArH_a), 7.342 (m, $J_{b\text{-}d}$ = 8.1 Hz, $J_{a\text{-}b}$ = 1.6 Hz; 2H, ArH_b), 7.277 (s, 4H, ArH_c), 6.900 (d, $J_{b\text{-}d}$ = 8.1 Hz, 2H; ArH_d), 3.856 (s, 6H, OCH_3).

Under the similar experimental procedures, *p*-phenylenediamine substituted with *o*-phenylenediamine or *m*-phenylenediamine, pink Compound B with mp of 220.4–220.8°C in a yield of 64%, or yellow Compound C with mp of 131.9–132.2°C in a yield of 72%, was prepared, respectively. FT-IR spectra of Compound B and C were shown in Figure 1(b,c).

^{1}H-NMR [DMSO-d_6, δ ppm, shown in Figure 1(e)] of Compound B: 9.608 (s, 1H, ArOH), 9.027 (s, 1H, ArOH), 7.719–7.657 (m, 1H, ArH_{b1}), 7.523–7.470 (m, $J_{b\text{-}d}$ = 8.1 Hz, $J_{a\text{-}b}$ = 1.6 Hz, 1H; ArH_{b2}), 7.285–7.130 (m, 4H, ArH_c), 6.910 (d, $J_{b\text{-}d}$ = 8.1 Hz, $J_{a\text{-}b}$ = 1.6 Hz, 1H; ArH_{d1}), 6.693–6.650 (m, $J_{b\text{-}d}$ = 8.1 Hz, $J_{a\text{-}b}$ = 1.6 Hz, 2H; ArH_{d2} and ArH_{a1}), 6.419–6.321(m, $J_{a\text{-}b}$ = 1.6 Hz, 1H; ArH_{a2}), 5.438 (s, 2H, N=CH), 3.713 (s, 3H, OCH_3), and 3.630 (s, 3H, OCH_3).

^{1}H-NMR [DMSO-d_6, δ ppm, shown in Figure 1(f)] of Compound C: 9.774 (s, 2H, ArOH), 8.531 (s, 2H, N=CH), 7.548 (d, $J_{a\text{-}b}$ = 1.6 Hz, 2H; ArH_a), 7.494 (m, $J_{b\text{-}d}$ = 8.1 Hz, $J_{a\text{-}b}$ = 1.6 Hz, 2H; ArH_b), 7.277 (m, 4H, ArH_c), 6.908 (d, $J_{b\text{-}d}$ = 8.1 Hz, 2H; ArH_d), 3.859 (s, 6H, OCH_3).

Preparation of Poly(conjugated azomethine-urethane)

7.52 g (0.020 mol) of Compound A was dissolved in 30 mL of DMF in a flask; 4.79 g (0.027 mol) of TDI was added subsequently. The reaction mixture was stirred at 40°C for 1 h and it gradually became a yellow viscous solution, and then the temperature was increased to 75–80°C before keeping it to continue to react for 2 h. DMF was removed by distillation under vacuum below 80°C under a nitrogen atmosphere. Thus, a yellow crude semisolid product (CAUP-A) was yielded and it was washed with ethyl acetate. This crude semisolid product was further purified with ethyl acetate in a Soxhlet apparatus for 2 h to remove some small molecule substances and oligomers. Finally, the refined yellow semisolid CAUP-A was dried in a vacuum oven under 1.33 k Pa at 40°C for 1 h before use. Likewise, light salmon pink CAUP-B and yellow CAUP-C were prepared using Compound B and Compound C, respectively, under the similar procedures.

Molecular weights and molecular weight distributions of CAUPs were measured by gel permeation chromatography (GPC) via a GPC instrument (series 200, Perkin Elmer, Perkin Elmer, Nicolet, Brookfield, and TA Instruments) using DMF as the eluent. The number-average molecular weights (M_n) of CAUP-A, CAUP-B and CAUP-C were determined to be 6.92 × 10^3, 5.69 × 10^3, and 5.59 × 10^3 g/mol, respectively; the molecular weight polydispersity indices (M_w/M_n, that is, weight–average molecular weight (M_w) versus M_n) of CAUP-A, CAUP-B and CAUP-C were 2.13, 1.97, and 2.29, respectively.

It is worthy to mention that the refined semisolid CAUPs should be immediately dissolved in DMF. Although the contents of —NCO functional groups in CAUPs are in the range of 1.16 × 10^{-3} ~1.32 × 10^{-3} mol/g, it should be pointed out that the semisolid CAUPs will become more and more hard solid because of the reaction of —NCO with moisture, and they cannot be dissolved in common organic solvents if they are exposed in air atmosphere for more than 10 h.

Preparation of Coating Film

The fresh refined semisolid CAUP was immediately dissolved in DMF with concentration of 30% weight fraction before a stoichiometric calculation amount of HPAR was added to prepare a polyurethane-polyacrylate coating solution. In preparing the DMF coating solution of HPAR/CAUP, CAUP and HPAR solutions were mixed based on 1 : 1 molar ratio of –NCO groups in CAUP versus —OH groups in HPAR. The coating films were prepared by coating the HPAR/CAUP solutions on clear and dry glass plates, and then the films were peeled off only when they were thoroughly dried in air atmosphere or in a heating condition at 120°C for 2 h.

Characterization Methods

FT-IR Test. FT-IR spectrum of Compound A, B, C, or CAUP in a KBr disk was performed in a spectrophotometer (360, Nicolet) in the spectral range of 450–4000 cm^{-1}, while FT-IR spectra of the film samples such as HPAR/CAUP-A, HPAR/CAUP-B and HPAR/CAUP-C were taken in an ATR method in

Applied Polymer SCIENCE

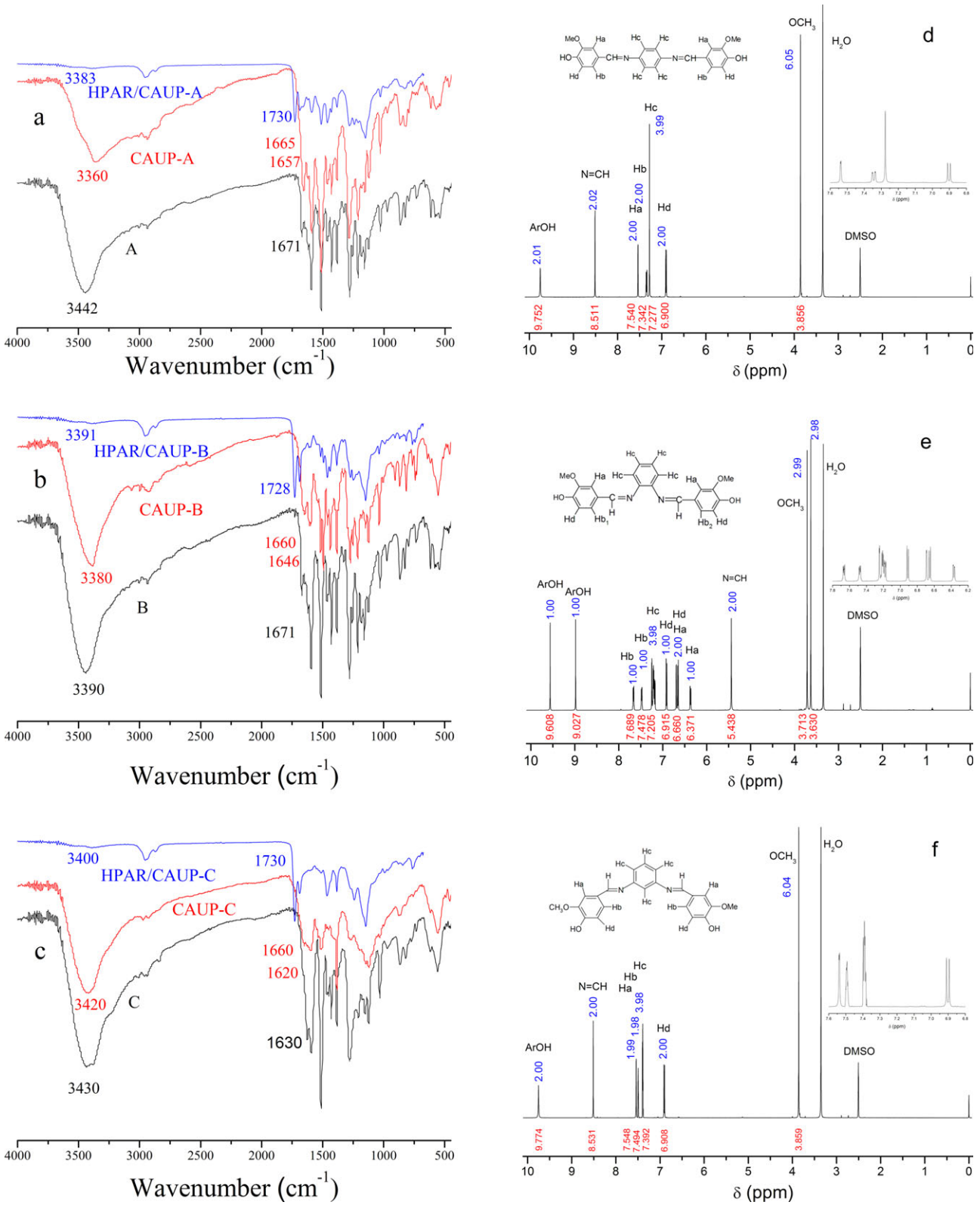

Figure 1. FT-IR (a–c) and ^{1}H-NMR (d–f) of A, B, and C, FT-IR of CAUPs and HPAR/CAUP films. [Color figure can be viewed in the online issue, which is available at wileyonlinelibrary.com.]

the spectral range of 675–4000 cm^{-1}, both methods were performed with a resolution of 4 cm^{-1} and 32 times of scanning.

^{1}H-NMR Test. ^{1}H-NMR spectra of Compound A, B and C were recorded with a 500 MHz NMR spectrometer (Avance III 500, Bruker, Swiss) by using DMSO-d_6 as a solvent at 25°C. Tetramethylsilane was used as internal standard.

Fluorescence Spectrum Test. The refined semisolid CAUPs were immediately dissolved in DMF at various concentrations. The fluorescence spectra of the CAUPs in dilute DMF solutions or the fluorescence spectra of HPAR/CAUP coating films were recorded using a fluorescence spectrofluorimeter (FL-4600, Hitachi, Japan) at room temperature in a scanning rate of 1200 nm/min and both excitation and emission slits were 5 nm.

Viscosity Measurement. A stoichiometric calculation amount of HPAR was added to the CAUP solution and mixed thoroughly to prepare a coating solution. After keeping at room temperature for 1 h, viscosity of the coating solution was measured by a viscometer (R/S Plus, Brookfield), a C50-1 cone (the diameter of 50 mm, cone angle of 1°) rotating for 30 s, in a single-point measuring method at 25°C in a shear rate of 50 s^{-1}.

UV–Vis Spectrum Test. A very dilute DMF solution of CAUP and HPAR/CAUP was coated out the wall of a quartz colorimetric cuvette, respectively. After the solvents were removed by drying, a very thin CAUP or HPAR/CAUP membrane was formed, respectively. Then the cuvette with a very thin membrane filled with anhydrous ethanol, which was as the reference vacant, was used to measure its UV–vis absorption spectrum, which was recorded using a UV–vis spectrophotometer (TU-1900, Beijing purkinje general instrument, China).

TGA. TGA of the coating film samples of HPAR/CAUPs were carried out using a TGA instrument (TGA/SDTA851e, Mettler-Toledo, Swiss). The film sample was measured from room temperature to 600°C at a heating rate of 10°C/min under a nitrogen atmosphere with a nitrogen gas flow of 50 mL/min.

DMTA Test. DMTA of the sample of HPAR/CAUP coating film was measured using a DMTA instrument (DMA Q800, TA Instruments) under nitrogen atmosphere at a heating rate of 2°C/min from 0 to 300°C.

Test Method of the Film Properties. According to the national standard method of China (GB/ T6739-2006, which is equivalent to ASTM D3363-2005), the pencil hardness value of the film on a standard tinplate was measured with a pencil hardness tester (QHQ, Tianjing Instrumental, China). The flexibility of the film on a standard tinplate was measured with a flexibility tester (QTX, Tianjing Instrumental, China) based on the national standard method of China (GB/T1731-1993, which is equivalent to ISO 1519-2002). According to the national standard of China (GB/T9754-2007, which is equivalent to ISO 2813-1994), the gloss value of the film on a standard tinplate was measured with a 60° incident angle specular gloss tester (QZX-60, Tianjing Instrumental Co., Tianjing, China).

RESULTS AND DISCUSSION

FT-IR, ^{1}H-NMR, and UV–Vis Analyses

FT-IR spectra of Compound A, B, and C, CAUPs and HPAR/CAUP films were shown in Figure 1. The stretching vibration absorption peaks of carbonyl groups in urethane linkages for CAUP-A and HPAR/CAUP-A [Figure 1(a)], CAUP-B and HPAR/CAUP-B [Figure 1(b)] and CAUP-C and HPAR/CAUP-C [Figure 1(c)] were found at 1665, 1660, and 1660 cm^{-1}, respectively. The absorption peaks in a vicinity of 1730 cm^{-1} for the coating films such as HPAR/CAUP-A, HPAR/CAUP-B and HPAR/CAUP-C were attributed to stretching and bend vibration of ester carbonyl groups in HPARs. Absorption peaks at 3360 cm^{-1} (CAUP-A) and 3383 cm^{-1} (HPAR/CAUP-A) in Figure 1(a), 3380 cm^{-1} (CAUP-B) and 3391 cm^{-1} (HPAR/CAUP-B) in Figure 1(b), and 3420 cm^{-1} (CAUP-C) and 3400 cm^{-1} (HPAR/CAUP-C) in Figure 1(c), and 1464 [Figure 1(a)], 1460 [Figure 1(b)] and 1460 [Figure 1(c)] cm^{-1} were attributed to stretching and bend vibration of N—H in urethane linkages; but the stretching and bend vibration of N−H in urethane linkages in the films of HPAR/CAUP-A, HPAR/CAUP-B and HPAR/CAUP-C were much weaker. 1281–1286 cm^{-1} band was attributed to C—O stretching vibration absorption; and the characteristic absorption peaks of azomethine (C=N) were found at 1657 and 1514 cm^{-1} [CAUP-A and HPAR/CAUP-A, Figure 1(a)], 1646 and 1516 cm^{-1} [CAUP-B and HPAR/CAUP-B, Figure 1(b)] and 1620 and 1510 cm^{-1} [CAUP-C and HPAR/CAUP-C, Figure 1(c)]. The 1593–1612 cm^{-1} band was attributed to aromatic ring vibration absorption. The characteristic peaks had hardly changed for azomethine (C=N) absorptions between CAUP-A and HPAR/CAUP-A, between CAUP-B and HPAR/CAUP-B and between CAUP-C and HPAR/CAUP-C, but they had red-shifted respectively by 14, 25, and 10 cm^{-1} compared with the FT-IR spectra of Compound A, B and C. These red-shifts suggested that CAUP-A, CAUP-B or CAUP-C, or HPAR/CAUP-A, HPAR/CAUP-B or HPAR/CAUP-C had stronger interactions than Compound A, B or C.

The ^{1}H-NMR spectrum [Figure 1(d)] of Compound A revealed it was a symmetrical molecule. δ of its azomethine protons was 8.511 ppm (s, 2H, N=CH), but it had strong intermolecaur interactions in DMSO-d_6 because its δ of phenolic hydroxyl groups (ArOH) was 9.752 ppm (s, 2H, ArOH). Other data of its ^{1}H-NMR were 7.540 ppm (d, $J_{a\text{-}b}$ = 1.6 Hz, 2H; ArH_a), 7.342 ppm (m, $J_{b\text{-}d}$ = 8.1 Hz, $J_{a\text{-}b}$ = 1.6 Hz, 2H; ArH_b), 7.277 ppm (s, 4H, ArH_c), 6.900 ppm (d, $J_{b\text{-}d}$ = 8.1 Hz, 2H; ArH_d), and 3.856 ppm (s, 6H, OCH_3).

^{1}H-NMR spectrum [shown in Figure 1(f)] of Compound C in DMSO-d_6 was similar to that of Compound A, which revealed Compound C was a symmetrical molecule, too. The chemical shift in 9.774 ppm (s, 2H, ArOH) and in 8.531 ppm (s, 2H, N=CH) were attributed to phenolic hydroxyl groups (ArOH) and azomethine protons, respectively. Other data of its ^{1}H-NMR were 7.548 ppm (d, $J_{a\text{-}b}$ = 1.6 Hz, 2H; ArH_a), 7.494 ppm (m, $J_{b\text{-}d}$ = 8.1 Hz, $J_{a\text{-}b}$ = 1.6 Hz, 2H; ArH_b), 7.277 ppm (m, 4H, ArH_c), 6.908 ppm (d, $J_{b\text{-}d}$ = 8.1 Hz, 2H; ArH_d), and 3.859 ppm(s, 6H, OCH_3).

The ^{1}H-NMR spectrum [Figure 1(e)] of Compound B revealed that there were strong intramolecular actions in the region of

the two *o*-amine groups of Compound B, resulting in that its δ of ArOH was 9.608 ppm (s, 1H, ArOH) and 9.027 ppm (s, 1H, ArOH). Because the two methoxyl groups had bigger steric hindrance, they had different δ values in 3.713 ppm (s, 3H, OCH_3) and in 3.630 ppm (s, 3H, OCH_3). Thus, its steric effect resulted in that the two H_b protons had chemical environmental inequality in different δ values of 7.719–7.657 ppm (m, 1H, ArH_{b1}) and 7.523–7.470 ppm (m, $J_{b\text{-}d} = 8.1$ Hz, $J_{a\text{-}b} = 1.6$ Hz, 1H; ArH_{b2}). Meanwhile, H_c, H_d, and H_a protons had respectively chemical environmental inequality with different δ values at 7.285–7.130 ppm (m, 4H, ArH_c), 6.910 ppm (d, $J_{b\text{-}d} = 8.1$ Hz, $J_{a\text{-}b} = 1.6$ Hz, 1H; ArH_{d1}), 6.693–6.650 ppm (m, $J_{b\text{-}d} = 8.1$ Hz, $J_{a\text{-}b} = 1.6$ Hz, 2H; ArH_{d2} and ArH_{a1}) and 6.419–6.321 ppm (m, $J_{a\text{-}b} = 1.6$ Hz, 1H; ArH_{a2}). Its δ value of azomethine protons was 5.438 ppm (s, 2H, N=CH).

CAUP-A, CAUP-B and CAUP-C had azomethine linkages that were known to have characteristic absorption bands in the UV–vis regions, in Figure 2, in which the normalized absorption intensity was used. The coating films of HPAR/CAUP-A, HPAR/CAUP-B and HPAR/CAUP-C were all transparent and had no absorption to visible light. All of those stronger UV-vis absorption bands of CAUP-A, CAUP-B or CAUP-C, and HPAR/CAUP-A, HPAR/CAUP-B or HPAR/CAUP-C coating film, appeared exactly at 209–420 nm that were attributed to $\pi \rightarrow \pi^*$ and $n \rightarrow \pi^*$ transitions that were consistent with Niu's study.[13] After DMF was removed by drying, a very thin CAUP or HPAR/CAUP membrane was formed out the cuvette. Because there were too many disturbing factors such as the effects of ethanol and DMF, air, moisture and film thickness and so on, therefore, the UV–vis spectra were more complicated in the shorter wavelength range of 200–250 nm, which could be clearly seen from Figure 2. In the range of 250–420 nm, the absorption peaks of CAUP-A, CAUP-B and CAUP-C were at 361, 298 and 285, 317 nm, respectively. Consequently, it could be concluded that CAUP-A had the highest molecular conjugation and symmetry because CAUP-A had the longest wavelength absorption peak. And in comparison to those of the CAUPs, the UV–vis absorption

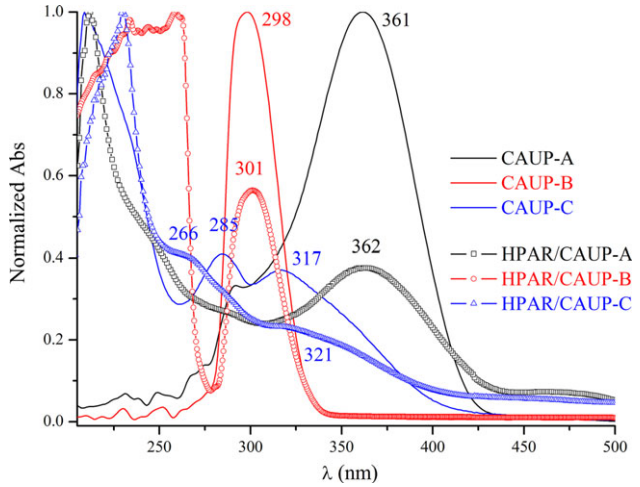

Figure 2. UV–vis absorption spectra of CAUPs and HPAR/CAUP coating films. [Color figure can be viewed in the online issue, which is available at wileyonlinelibrary.com.]

peaks of HPAR/CAUP-A, HPAR/CAUP-B and HPAR/CAUP-C films were also red-shifted by 1–4 nm, red-shifting to 362, 301, and 321 nm, respectively. Obviously, these absorptions were not sensitive enough. Both Ambrozic and Zigon[14] and Lewinski et al.[15] reported that intermolecular or intramolecular interactions such as polar interactions or hydrogen bonds could cause to absorption red-shift phenomena. Because there were many proton donor species such as amine and azomethine groups in CAUPs, meanwhile there also were many proton acceptor species such as nitrogen atoms in azomethine, urethane, amide groups and carbonyl groups in CAUPs. These species perhaps were assumed to be polar interactions or hydrogen bonds, which might cause absorption red-shift. So, it was necessary to investigate their fluorescence spectra of CAUPs.

Fluorescence Analysis and Intermolecular and Intramolecular Interactions

DMF solutions of CAUP-A, CAUP-B, and CAUP-C were excited with UV and then their $\pi^* \rightarrow \pi$ transitions emitted fluorescence. Their fluorescence excitation and emission spectra were shown in Figure 3. By analyzing further the fluorescence excitation and emission spectra of CAUP solutions, we had found that there were red shift phenomena. These red shift phenomena of emission spectra of CAUP solutions also suggested that they could change higher energy UV into lower energy ones. With different CAUP-A concentration from 3.20×10^{-5} to 8.00 g/L, as the CAUP-A solutions were excited with UV excitation wavelength (λ_{ex}) of 287 nm [Figure 3(a-1)], 351 nm or 358 nm [Figure 3(a-2)], the emission wavelength (λ_{em}) values of the fluorescence emission spectra were in 341–352 nm [Figure 3(a-1)], 399–402 nm and 423–427 nm [Figure 3(a-2)], respectively. Figure 3(a-2) showed that the CAUP-A solution had longer λ_{ex} values of 351 and 358 nm and gave longer λ_{em} values in 399–402 nm and 423–427 nm [Figure 3(a-2)], respectively. But the intensity of its fluorescence emission in 399–402 or 423–427 nm was much weaker than that in 341–352 nm. Because CAUP-A had more symmetrical molecular structure, this might easily result in that CAUP-A segment formed longer intermolecular segmental stacks.[15–18] Meanwhile, CAUP-A segment in dilute solution could rotate by encircling its molecular symmetrical axis, its rigidity would be descent. Hence, CAUP-A solution might generate much weaker fluorescence intensity in a longer wavelength range of 399–402 or 423–427 nm.

With regard to CAUP-B solutions in the concentration range of 3.20×10^{-5}–0.800 g/L, 290 nm was used as λ_{ex} to excite CAUP-B solutions, their λ_{em} values were gradually red-shifted from 355 to 369 nm [Figure 3(b)]. The emission spectra of CAUP-C solutions in the concentration range of 1.00×10^{-3}–1.00 g/L, in Figure 3(c), the λ_{em} value was red-shifted from 325, 359 to 374 nm while its λ_{ex} value was 289, 299, and 310 nm, respectively. It was noticeable that the intensity of their fluorescence emission of either CAUP-A or CAUP-C solution was weaker than that of CAUP-B solution. This was caused by the strongest CAUP-B intramolecular hydrogen bonding effects. To make a comparison between the different species in a clear manner, we compared the fluorescence spectra in a term of the normalized intensity. All red-shift phenomenon data were shown in Figure 3 and their comparisons were listed in Table II.

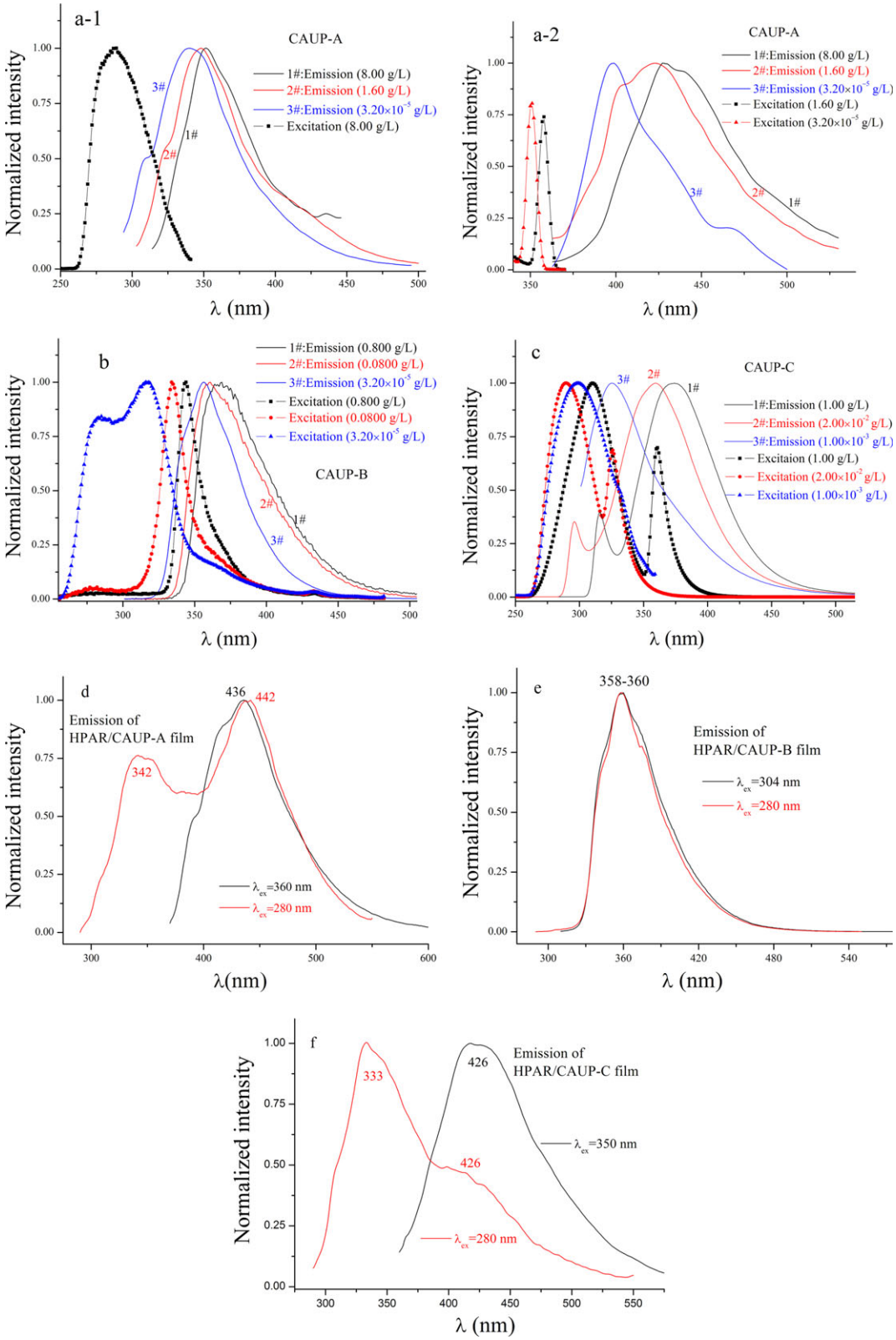

Figure 3. Fluorescence spectra of DMF solutions of CAUPs (a-1, a-2, b, and c) and the films of HPAR/CAUPs (d–f). [Color figure can be viewed in the online issue, which is available at wileyonlinelibrary.com.]

Table II. The Fluorescence Spectrum Change Comparison of CAUP Solution in Different Concentration

CAUP	Concentration (g L^{-1})	Emission spectrum			Excitation spectrum
		λ_{ex} (nm)	λ_{em}(nm)	$\Delta\lambda_{emr}$(nm)	λ_{exm}(nm)
CAUP-A	3.20×10^{-5}	287	341	34	287
	3.20×10^{-4}	287	343	36	287
	0.160	287	345	34	287
	1.60	287	348	35	287
	8.00	287	352	36	287
	3.20×10^{-5}	351	399	33	351
	3.20×10^{-4}	351	402	37	351
	0.160	358	401	41	358
	1.60	358	423	42	358
	8.00	358	427	48	358
CAUP-B	3.20×10^{-5}	290	355	29	277
	3.20×10^{-4}	290	356	29	283
	3.20×10^{-3}	290	356	30	316
	3.20×10^{-2}	290	358	33	329
	0.0800	290	361	40	334
	0.800	290	369	39	344
CAUP-C	1.00×10^{-3}	289	325	38	289
	2.00×10^{-2}	299	359	37	299
	1.00	310	374	40	310

From Table II, the excitation wavelength (λ_{exm}) values with the strongest intensity in excitation spectra became bigger and bigger with concentration increase. Interestingly, with concentration increase, the λ_{em} values of CAUP-A, CAUP-B, and CAUP-C solutions were all gradually red-shifted. This could be attributed to the fact that there were many π conjugations in the backbone of CAUPs and many intermolecular and intramolecular interactions of D-π-A and hydrogen bonds[17] which might cause CAUP molecule aggregations.

In the concentration range of 3.20×10^{-5}–3.20×10^{-3} g/L, the peaks of emission spectra of CAUP-B solutions were almost at 356 nm. It was observed that there were 6–11 nm of emission red-shift in the concentrated solution (0.0800–0.800 g/L) compared with that of the dilute solutions (3.20×10^{-5}–3.20×10^{-3} g/L). We assumed that the greater emission spectral changes at higher concentration conditions might be related to its higher intermolecular and intramolecular hydrogen bonding effects. In addition, because the emission spectrum of the concentrated solution was a mirror image of the excitation spectrum, it indicated that the absorbing and emitting species were in the same probable molecule electronic states. However, the emission spectrum changes of CAUP-B solutions were not dependent on λ_{ex} values. Taking the CAUP-B solution with a concentration of 3.20×10^{-5} g/L as an example, we found that while different λ_{ex} values ranging from 275 nm to 320 nm by an interval of 5 nm were used to excite the fluorescence, the λ_{em} values of CAUP-B solution were all at 355 nm.

It could be easily seen that the fluorescence spectrum curves of CAUP solutions were all deviated from the normal distribution curve. When the normalized intensity was 0.5, there was a point on the right side of the fluorescence emission spectrum curve, at which the emission wavelength value (λ_{emr}) on the right side could be read out. Thus, a deviation value could be calculated as $\Delta\lambda_{emr} = \lambda_{emr} - \lambda_{em}$. From Table II, with concentration increase, the $\Delta\lambda_{emr}$ values of CAUP-A, CAUP-B, and CAUP-C solutions were all gradually increased.

These red shift phenomena were consistent with their viscosity data at 25°C when the concentrations of those solutions were increased. Viscosity of HPAR/CAUP-A solution increased from 0.0508 to 0.300 Pa·s when its concentration increased from 0.160 to 1.60 g/L. Viscosity of HPAR/CAUP-B solution increased from 0.0728 to 0.210 Pa·s as its concentration increased from 3.20×10^{-3} to 0.0800 g/L. Viscosity of HPAR/CAUP-C solution increased from 0.0618 to 0.180 Pa·s as its concentration increased from 1.00×10^{-3} to 1.00 g/L. However, the viscosity of such a dilute HPAR solution was not increased with its concentration increase. So, CAUP molecules aggregated in the concentrated solution and supramolecular actions were enhanced because of the CAUP intermolecular segmental stacks.

Fluorescence emission spectra of the films of HPAR/CAUP-A, HPAR/CAUP-B and HPAR/CAUP-C were shown in Figure 3(d–f), respectively. 280 nm UV was used to excite them, the film of HPAR/CAUP-A gave λ_{em} values of 342 and 442 nm; the film of HPAR/CAUP-C gave λ_{em} value of 333 nm, respectively. As excitation wavelength of 360 or 350 nm was severally used to excite them, the film of HPAR/CAUP-A and HPAR/CAUP-C gave λ_{em} values of 436 and 426 nm, respectively. However, λ_{em} value of the film of HPAR/CAUP-B was 358–360 nm when either 280 or

304 nm UV to excite it. As the excitation intensity was a fixed value and the intensity of the fluorescence emission spectrum was recorded in photon counts, the intensity of the fluorescence emission spectrum of HPAR/CAUP-B film was strongest. For comparison, their fluorescence intensity was still shown in the normalized intensity. Although it was difficult to distinguish their fluorescence spectra how to depend on thickness (concentrations of CAUPs) of the films, it was showed that their fluorescence emission spectra actually depended on excitation wavelength and they had UV-converting abilities for converting higher energy UV rays to lower energy ones.

Mechanical and Thermal Properties of the Coating Films

On the basis of the matrix polymers of HPAR/CAUPs or HPAR/HDI, some transparent coating films were prepared. It was worthy to mention that the HPAR/CAUP solutions were prepared using DMF as solvent since CAUPs could not be dissolved in other common organic solvents such as toluene, xylene, cyclohexanone or butyl acetate, and so forth. In the anti-UV irradiation and anti- experiments, it was required that the polyurethane coating film had sufficient mechanical properties and it would be more welcome if its glass transition temperature could be above 60°C. The compatibility among polyurethane coating film layers were excellent so that the film layers could enforce each other and they had an excellent adhesive property, which allowed them to be well attached to substrate materials such as glass, iron and wood, etc. Certainly, the HPAR/CAUP films owned a strong mechanical strength and 4 H to 5 H pencil hardness after they were dried in air atmosphere for a certain time or in a heating condition. Besides, the HPAR/CAUP films which met 1 mm of flexura possed a good flexibility. Hence, such good mechanical properties of the three HPAR/CAUP films allowed them to be candidates for coating films.

The elastical storage moduli (E') of the HPAR/CAUP films were over 10^{10} Pa and the elastical loss moduli (E'') were over 10^9 Pa when they were in the glassy state. During DMTA testing of thermodynamic properties of HPAR/CAUP coating film, it showed several peaks, but there was only one peak at which $\tan\delta_T$ ($\tan\delta_T = E''/E'$) had the maximum value. In this peak vicinity of $\tan\delta_T$ curve versus temperature, the modulus of HPAR/CAUP coating film declined more than 10^3 M Pa with increasing temperature. According to DMTA analysis, here the glass transition temperature (T_g) of the HPAR/CAUP coating film was reported as the temperature at which $\tan\delta_T$ was the maximum.[7,19] From Figure 4, T_gs of the three HPAR/CAUP film samples were all over 97.0°C, among which the T_g of the HPAR/CAUP-B film was the highest. This was consistent with that the fluorescence intensity of HPAR/CAUP-B film or CAUP-B solution was the strongest in the three candidates, which resulted from the highest rigidity in the CAUP-B intramolecular structure. This was because there were more intramolecular hydrogen bonding effects in the region of the two *ortho*-amines of CAUP-B than that in CAUP-A and CAUP-C. Conversely, the molecular symmetry of CAUP-A was the best followed by that of CAUP-C, and this seemed to the cause of the greater stacking and hydrogen bonding effects existing in CAUP-A. However, the intermolecular stacking of HPAR/CAUP-A or HPAR/CAUP-C might be negatively weakened by HPAR segments. Thus, the T_g of HPAR/CAUP-B film was the highest.

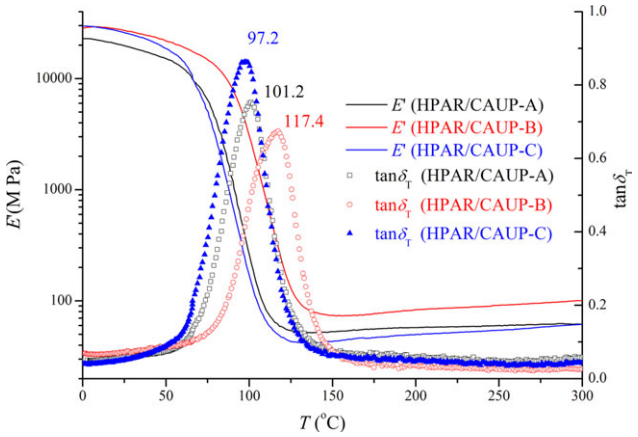

Figure 4. DMTA of the samples of HPAR/CAUP coating films. [Color figure can be viewed in the online issue, which is available at wileyonlinelibrary.com.]

Furthermore, DMTA also indicated that they were all in the glassy state below 97°C and the HPAR/CAUP films had high moduli. As a result, HPAR/CAUP films had higher pencil hardness values of 4 H–5 H. When temperature was over 100°C, the film materials became probably in the rubber elastic state, however, their E' were still over 10^7 Pa.

T_g and E' of HPAR/HDI coating films[7,20] were below 55.9°C and 10^9 Pa, respectively. Compared with HPAR/HDI coatings, the HPAR/CAUP coating films had higher glass transition temperature, which were over 97.0°C. This meant that HPAR/CAUP coating films had a higher upper limit of use temperature.

The TGA and derivative thermogravimetric (DTG) analyses of the HPAR/CAUP film samples were shown in Figure 5. The small weight loss observed below 108.0°C might be caused by the adsorptive water and moisture. From 108.0 to 244.7°C in Figure 5(a), there was 19.0–20.0% of weight loss, which was attributed to the thermal degradation of urethane segments as reported in the literature.[21,22] In particular, the temperatures corresponding to 10% of weight loss for the sample films of HPAR/CAUP-A, HPAR/CAUP-B, and HPAR/CAUP-C were at 177.1, 169.7, and 260.0°C, respectively. As a matter of fact, in a polyurethane coating of HPAR/CAUPs, there were more complex hydrogen bonding and stacking effects in CAUP segments than in HPAR segments and the difference of the degradation temperatures for these three polyurethane coating films were significantly related to the difference of such hydrogen bonding and stacking effects existing in these three different CAUP segments. Particularly, there was more intramolecular hydrogen bonding effects in CAUP-B segment than that in CAUP-A and CAUP-C segments. On the other hand, there was a better molecular symmetry in the axis direction of the two *para*-amine groups in CAUP-A or in the axis direction of the two *meta*-amine groups in CAUP-C, which resulted in greater intermolecular stacking and hydrogen bonding effects in CAUP-A and CAUP-C than in CAUP-B segment. In the solution, CAUP-A might rotate by encircling its molecular symmetrical axis such

Applied Polymer SCIENCE

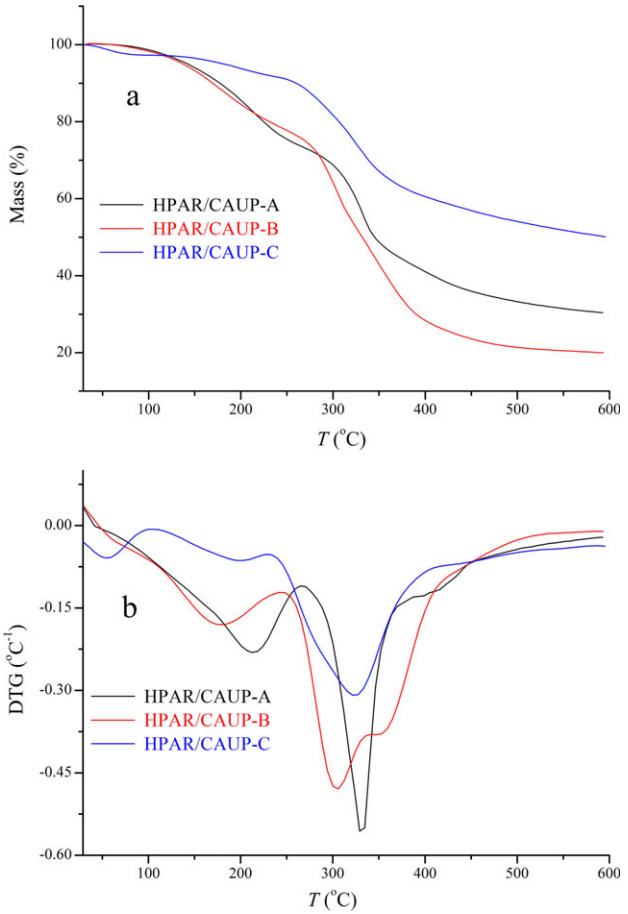

Figure 5. TGA (a) and DTG (b) of HAPR/CAUP coating film samples. [Color figure can be viewed in the online issue, which is available at wileyonlinelibrary.com.]

as the direction of *para*-amine groups, and this rotation might enwind a few of HPAR soft segments into HPAR/CAUP-A, which could reduce its hydrogen bonding and stacking effects. As a result, HPAR/CAUP-A reduced its degradation temperature. Consequently, the degradation temperature of HPAR/CAUP-A film was lower than that of HPAR/CAUP-C but higher than that of HPAR/CAUP-B. Furthermore, in the higher temperature range of 244.7–409.7°C, the weight loss was found to be around 46.0–50.9%. This was attributed to thermal degradation of Compound A-like, Compound B-like or Compound C-like linkages in CAUPs and that of HPAR thermal degradation. The above TGA data demonstrated that these HPAR/CAUP films also had high enough thermal degradation temperatures.

DTG revealed that the first temperature (T_{max})[19,21] corresponding to the maximum thermal degradation velocity of HPAR/CAUP-A, HPAR/CAUP-B and HPAR/CAUP-C film sample, Figure 5(b), was at 212.3, 176.0, and 201.1°C, respectively. In the higher temperature range of 244.7–409.7°C, the second T_{max} of HPAR/CAUP-A, HPAR/CAUP-B and HPAR/CAUP-C film sample was at 329.0, 308.1, and 321.6°C, and their third T_{max} was at 402.5, 341.5, and 432.7°C, respectively.

UV-Converting Application of HPAR/CAUP Films

The fluorescence excitation and emission spectra demonstrated that CAUPs and HPAR/CAUP films had the functional abilities of changing higher energy (shorter wavelength) UV rays into lower ones (longer wavelength). From Figure 3, their excitation wavelengths were all longer than 280 nm and these data revealed that CAUPs could absorb those UV rays. The natural UV rays reaching the earth are UV-A band and UV-B band rays that their wavelengths are longer than 280 nm. If polymer materials are applied to natural exposure, they can severely be deteriorated by those shorter wavelength UV rays in UV-A and UV-B rays. In our application work, CAUPs were used as a hard component in the HPAR/CAUP polyurethane coatings to be coated on those surfaces of red or phthalocyanine blue color decorative film materials which were sensitive to shorter wavelength UV rays. Hence, the natural lives of the complex color decorative films were increased because they changed shorter wavelength UV into longer ones. The HPAR/CAUP coating film was actually applied as a UV-converting mid-film. Finally, HPAR/HDI coating film used as a finish film was coated on the HPAR/CAUP mid-film. Thus, a complex color film with UV-converting abilities was prepared in this way in our practical application. Under natural exposure to ageing in Lhasa for more than 9 months, the applied results showed that the gloss changes of the complex red or blue films were from an original gloss value of 95% to a retention gloss value of over 92%. As a result, the anti-photodegradation and anti-photo properties of the complex red or blue films were more excellent than that of the pure HPAR/HDI film.[7]

CONCLUSIONS

CAUPs with three different aromatic structures were prepared and they had been demonstrated to have no absorption in the visible light wavelength range. The CAUP solutions were able to be excited with shorter wavelength UV and thereafter they could emit longer wavelength rays. Besides, their fluorescence emission spectra in higher concentrated solutions had red-shift phenomena because there were many molecule stacks and aggregations through intermolecular and intramolecular D-π-A and hydrogen bond interactions. CAUPs used as hard segments, meanwhile HPAR used as a soft segment, transparent HPAR/CAUP coating films were prepared, which had either no absorption in the visible light wavelength range. More interestingly, the HPAR/CAUP coatings had functional abilities of converting higher energy UV rays to lower energy ones, which enabled them to have potential application in severe high UV conditions.

Moreover, the DMTA and TGA data of the HPAR/CAUP coating films revealed that they had good mechanical properties and high enough thermal properties as well as high glass transition temperatures. However, the thermal degradation temperatures of the three HPAR/CAUP films were quite different due to the difference of the complicated intermolecular and intramolecular interactions in their CAUP segments in solid state.

This work was supported by Natural Science Foundation of Fujian Province of China (No. 2012J01030). The authors thank Mr Huagui Zhang for his dedication in this paper.

REFERENCES

1. Buruiana, E. C.; Olaru, M.; Strat, M.; Strat, G.; Simionescu, B. C. *Polym. Int.* **2005**, *54*, 1296.
2. Liou, G.-S.; Lin, H.-Y.; Hsieh, Y.-L.; Yang, Y.-L. *J. Polym. Sci. A: Polym. Chem.* **2007**, *45*, 4921.
3. Siling, S. A.; Shamahin, S. V.; Ronova, I. A.; Kovalevski, A. Y.; Grachev, A. B.; Tsiganova, I. Y.; Yuzhakov, V. I. *J. Appl. Polym. Sci.* **2001**, *80*, 398.
4. Issam, A. M.; Ismail, J. *J. Appl. Polym. Sci.* **2006**, *100*, 1198.
5. Bajsic, E. G.; Rek, V. *J. Appl. Polym. Sci.* **2001**, *79*, 864.
6. Kaya, I.; Yildirim, M.; Kamaci, M.; Avci, A. *J. Appl. Polym. Sci.* **2011**, *120*, 3027.
7. Liu, C.-P. *J. Appl. Polym. Sci.* **2007**, *104*, 1271.
8. Cheong, M. Y.; Ooi, T. L.; Ahmad, S.; Yunus, W. M. Z. W.; Kuang, D. *J. Appl. Polym. Sci.* **2009**, *111*, 2353.
9. Kapole, S. A.; Kulkarni, R. D.; Sonawane, S. H. *Can. J. Chem. Eng.* **2011**, *89*, 1590.
10. Pickett, J. E.; Moore, J. *Polym. Deg. Stab.* **1993**, *42*, 231.
11. Goncalves, V. C.; Carvalho, A. J. F.; Balogh, D. T. *Polym. Int.* **2010**, *59*, 637.
12. So, Y.-H. *Polym. Int.* **2006**, *55*, 127.
13. Niu, H. J.; Huang, Y. D.; Bai, X. D.; Li, X. *Mater. Lett.* **2004**, *58*, 2979.
14. Ambrozic, G.; Zigon, M. *Polym. Int.* **2005**, *54*, 606.
15. Lewinski, J.; Zachara, J.; Justyniak, I.; Dranka, M. *Coord. Chem. Rev.* **2005**, *249*, 1185.
16. Peng, K.-Y.; Chen, S.-A.; Fann, W.-S. *J. Am. Chem. Soc.* **2001**, *123*, 11388.
17. Simas, E. R.; Akcelrud, L. *J. Lumin.*. **2003**, *105*, 69.
18. Machado, A. M.; Munaro, M.; Martins, T. D.; Dvila, L. Y. A.; Giro, R.; Caldas, M. J.; Atvars, T. D. Z.; Akcelrud, L. C. *Macromolecules* **2006**, *39*, 3398.
19. Chattopadhyay, D. K.; Rohini Kumar, D. B.; Sreedhar, B.; Raju, K. V. S. N. *J. Appl. Polym. Sci.* **2004**, *91*, 27.
20. Liu, C.-P.; Lin, J.-H.; Lin, Y.-S. *J. Fujian Normal Univ. (Nat Sci Ed)* **2008**, *24*, 52.
21. Chen, X.; Hu, Y.; Jiao, C.; Song, L. *Polym. Degrad. Stab.* **2007**, *92*, 1141.
22. Dutta, S.; Karak, N. *Polym Int* **2006**, *55*, 49.